

Article

An Improved Combination Model for the Multi-Scale Prediction of Slope Deformation

Xiangyu Li ¹, Tianjie Lei ^{2,*}, Jing Qin ^{1,*}, Jiabao Wang ^{3,†}, Weiwei Wang ^{4,†}, Dongpan Chen ^{5,†}, Guansheng Qian ^{2,†} and Jingxuan Lu ¹ 

¹ State Key Laboratory of Simulation and Regulation of Water Cycle in River Basin, China Institute of Water Resource and Hydropower Research, Beijing 100038, China

² Institute of Environment and Sustainable Development in Agriculture, Chinese Academy of Agricultural Sciences, Beijing 100081, China

³ College of Geoscience and Surveying Engineering, China University of Mining and Technology (CUMTB), Beijing 100083, China

⁴ China Electronic Greatwall ShengFeiFan Information System Co., Ltd., Beijing 102200, China

⁵ Faculty of Information Technology, Beijing University of Technology, Beijing 100124, China

* Correspondence: leitianjie@caas.cn (T.L.); qinjing@iwahr.com (J.Q.); Tel.: +86-108-210-5990 (T.L.)

† These authors contributed equally to this work.

Abstract: Slope collapse is one of the most severe natural disaster threats, and accurately predicting slope deformation is important to avoid the occurrence of disaster. However, the single prediction model has some problems, such as poor stability, lower accuracy and data fluctuation. Obviously, it is necessary to establish a combination model to accurately predict slope deformation. Here, we used the GFW-Fisher optimal segmentation method to establish a multi-scale prediction combination model. Our results indicated that the determination coefficient of linear combination model, weighted geometric average model, and weighted harmonic average model was the highest at the surface spatial scale with a large scale, and their determination coefficients were 0.95, 0.95, and 0.96, respectively. Meanwhile, RMSE, MAE and Relative error were used as indicators to evaluate accuracy and the evaluation accuracy of the weighted harmonic average model was the most obvious, with an accuracy of 5.57%, 3.11% and 3.98%, respectively. Therefore, it is necessary to choose the weighted harmonic average model at the surface scale with a large scale as the slope deformation prediction combination model. Meanwhile, our results effectively solve the problems of the prediction results caused by the single model and data fluctuation and provide a reference for the prediction of slope deformation.

Keywords: prediction; combination model; fisher optimal segmentation; goodness-of-fit weight; multi-scale; high slope



Citation: Li, X.; Lei, T.; Qin, J.; Wang, J.; Wang, W.; Chen, D.; Qian, G.; Lu, J. An Improved Combination Model for the Multi-Scale Prediction of Slope Deformation. *Water* **2022**, *14*, 3667. <https://doi.org/10.3390/w14223667>

Academic Editors: Weiwei Shao, Zhaohui Yang and Xichao Gao

Received: 30 September 2022

Accepted: 9 November 2022

Published: 14 November 2022

Publisher's Note: MDPI stays neutral with regard to jurisdictional claims in published maps and institutional affiliations.



Copyright: © 2022 by the authors. Licensee MDPI, Basel, Switzerland. This article is an open access article distributed under the terms and conditions of the Creative Commons Attribution (CC BY) license (<https://creativecommons.org/licenses/by/4.0/>).

1. Introduction

High slope collapse is one of the most destructive and costly natural disasters. Flood and rainwater disasters easily cause slope collapse and landslides in mountainous areas. Once the slope collapses, the disasters will have a serious impact on the safety of water engineering, water resource, ecology and society [1–5]. China has faced long-lasting and severe collapse disasters in the past. The influences of collapse disasters have evoked high levels of interest outside of the scientific community. Therefore, establishing the appropriate prediction models to accurately predict slope deformation in time is important to ensure safety and to avoid the collapse disasters in the process of constructing water engineering [6–10].

In recent years, the time-series model and the artificial intelligence model are used by most scholars and they have become an important means of slope deformation prediction because of its strong stability, high accuracy and good applicability. Among them, the time-series model can mainly analyze the historical data, which then finds the rule of data

development, and predicts the data in the future [11–15]. As a branch of computer science, artificial intelligence technology has been gradually applied for prediction in the field of slope deformation by many scholars in recent years, and mainly include the ANN model and SVR model [16–20]. At present, the time-series model and the artificial model have focused on deformation prediction in the field of slope collapse disasters [21–23]. Nevertheless, some scholars have noted that the single prediction model has some limitations in predicting deformation for high slope, such as failing to identify the abrupt points of deformation and to show the linear and nonlinear trend of slope deformation [24,25]. To overcome these limitations, some scholars proposed the combination model to predict slope deformation. The combination model could solve the shortcomings of the single model and adequately combine the advantages of the single model as a new method for predicting slope deformation [26,27]. Nevertheless, the combination model proposed by present studies have revealed a variety of errors caused by unsteady data trends and severe data fluctuation, but few studies have considered the impact of these factors on the stability of the combination prediction models. Meanwhile, the weight of the single model could be affected by the human factor. Accordingly, the combination model could be further modified to improve the prediction accuracy of predicting deformation.

While most scholars have discussed the application of the combination model in the field of predicting the slope deformation, the influence of unsteady data trends, data fluctuation and human factor on the prediction results has not been effectively solved [28,29]. What we need is a process to predict the slope deformation and to solve the interference of unsteady data trends and data fluctuation, as well as assign the objective weight for the single model to ensure the accuracy of the prediction results. Here, we collected the data of “day” time scale, including deformation speed, deformation acceleration and deformation data in Hongshiyuan water project, and proposed the modified combination prediction model. Based on the traditional method, the sample data were segmented through the Fisher optimal segmentation model, and the Machine Learning models were then used to predict the segmented data, so as to solve the interference of unsteady data trends and severe data fluctuation. Meanwhile, the goodness of fit of the model as the basis of evaluating the suitability of the model could evaluate the quality of the prediction model well, and the GFW model was used to calculate the weights of the different single model, from which the combination model was constructed. The technical route of the method is shown in Figure 1. This solves the limitation of the traditional prediction models, which can be interfered with by the human factor and data fluctuation. Compared to previous studies, our proposed method can better improve the prediction ability and provide a simple, efficient and new method for slope deformation prediction.

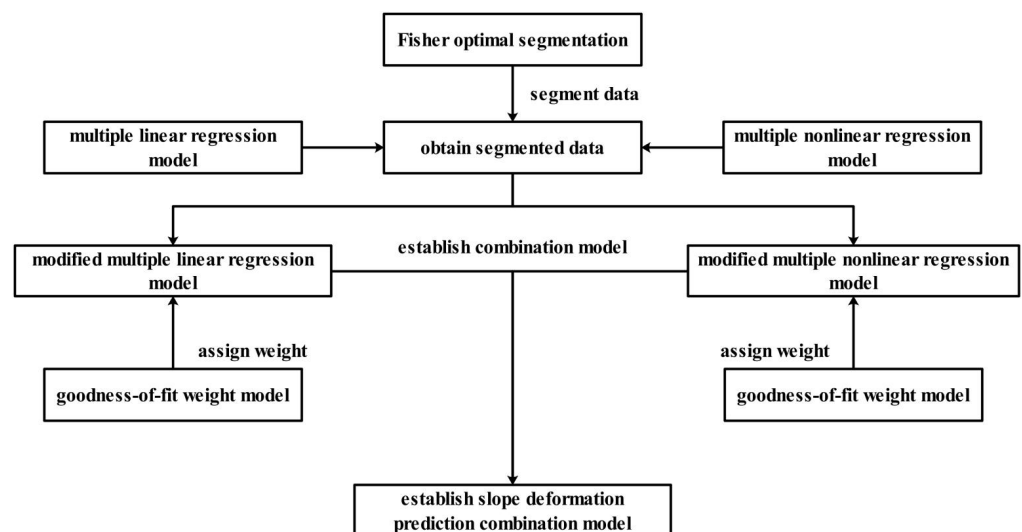


Figure 1. The technical route of the modified slope deformation prediction combination model.

2. Materials and Methods

2.1. Study Area

The study area is a high slope of the Hongshiyuan water control project. The project is a key project of the overall plan of the State Council for post-earthquake restoration in Ludian City. It is also the largest single project for post-earthquake restoration and reconstruction in Ludian City. The Hongshiyuan dammed lake renovation project is an important project to control water hazards in China, and it is also one of the representative and important projects in the international water conservancy and hydropower industry [30–32]. The overview of the study area is shown in Figure 2.

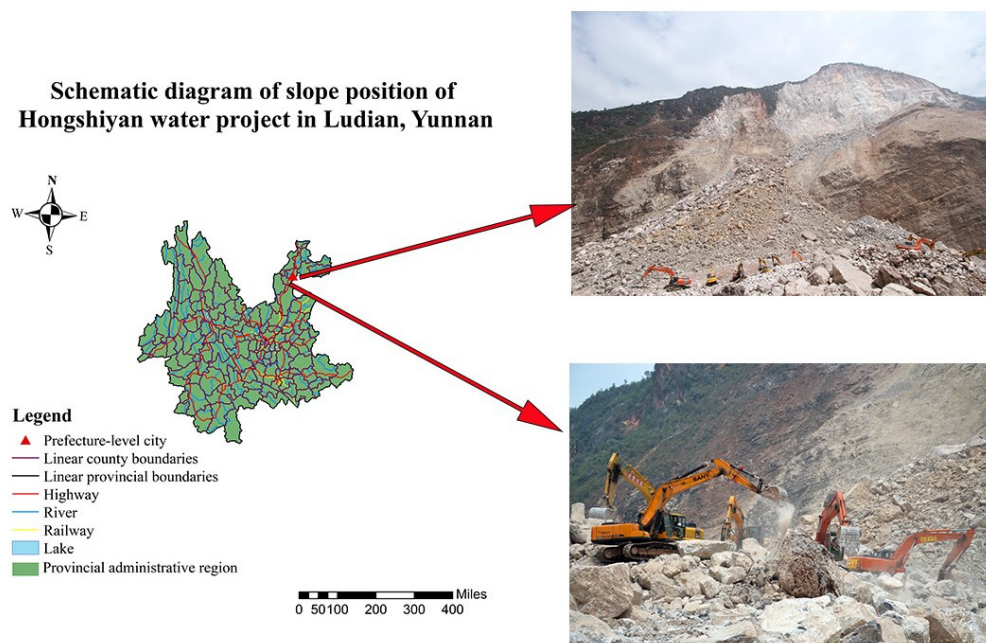


Figure 2. The location of the slope of the Hongshiyuan water project.

The slope is a typical rock slope with no vegetation cover, large height drop and steep terrain. The slope was formed by the collapse of the mountain caused by the earthquake with a magnitude 6.5 on 3 August 2014 [33]. According to the survey of the downstream side of the slope, the geological conditions of the excavation periphery are delineated for dangerous rock mass. The dangerous rock mass of the slope is mainly divided into class I and class II, the dangerous rock area of class I is mainly characterized by two groups of steep incline fissure cuts of parallel slope and vertical slope, and the width of gap is large and basically separated from the slope surface, and the stability is extremely poor. The dangerous rock area of class II is mainly characterized by two groups of steep incline fissure cuts of parallel slope and vertical slope, the width of the gap is short and dense, but the width is not large, and the stability is poor [34–36]. Meanwhile, the conditions of the project are complex with continuous aftershocks during the construction process and accompanied by severe weather such as heavy rainstorms. Therefore, to ensure the safety of the construction and operation of the Hongshiyuan water project, it is necessary to strengthen the prediction of the slope deformation.

2.2. Data Source

The data source in this study are mainly from Ground-based Synthetic Aperture Radar technology, UAV Remote Sensing technology and field survey technology. The deformation data, deformation speed data and deformation acceleration data were both from Ground-based Synthetic Aperture Radar technology. Among them, Ground-based Synthetic Aperture Radar is a high-resolution radar, which is characterized by a high

resolution ratio, large scale and enabling real-time automatic monitoring of all-day and all-weather, and the radar should be obtained by high-resolution radar images under villainous environmental conditions. The data of each grid could be obtained by data processing and the accuracy could reach sub millimeter [37,38]. Additionally, the DEM data were from UAV Remote Sensing technology and field survey technology, it also mainly obtained the deformation data, deformation speed and deformation acceleration at different scales. To ensure we obtained multi-scale data, we used the method of mathematics statistics to count and handle the data from Ground-based Synthetic Aperture Radar technology. We took slope deformation data as an example. The point deformation is the largest deformation of all segmented grids in the high slope DEM model. The linear deformation is the sum of all segmented grids of terrain lines in the high slope DEM model. The surface deformation is the sum of all segmented grids deformed in the same direction in the high slope DEM model. Finally, we used the method of mathematics statistics to handle the deformation data at other spatial scale such as the linear scale and surface scale.

2.3. Multiple Linear Regression Model

The relationship between the human factor, geological factor, environmental factor and other multi-source factors may be independent, contained or interactive. Under ideal conditions, slope deformation may have a significant linear relationship with the human factor, geological factor and environmental factor. Therefore, the multiple regression model is used to complete the linear prediction of slope deformation.

The linear regression model is the study of the mapping and mutual relationship between two variables, and the method of measuring the closeness and quantitative relationship between two variables [39–43]. Thus, the regression relationship between two variables is often called the linear regression model. Meanwhile, the regression relationship between more variables is called the multiple linear regression model, and the model is used to analyze the regression relationship between a dependent variable and more independent variables.

In this study, the main factors affecting slope deformation were divided into human factors, meteorological factors, and geological factors, etc. The multiple linear regression of the slope deformation can be expressed as follows:

$$y_1 = \beta_0 + \beta_1x_1 + \beta_2x_2 + \dots + \beta_nx_n + \varepsilon \quad (1)$$

where y_1 represents the predicted results of using a multiple linear regression model, $x_1, x_2 \dots x_n$ are the factors that affect the slope deformation, $\beta_0, \beta_1, \beta_2, \dots, \beta_n$ are the coefficients, and ε is the random error.

2.4. Multiple Nonlinear Regression Model

However, in practical application, slope deformation is often affected by the human factor, geological factor, environmental factor and other multi-source factors. The relationship between deformation and multi-source factors should not be independent, and their relationship approximately presents the nonlinear relationship. Meanwhile, the multiple linear regression model is only appropriate for sufficient sample data, and it is difficult to fit sufficient sample data quickly for the multiple linear regression model. The response relationship between deformation and external factors is more complicated, and when slope deformation is fluctuated strongly in the certain factors, the response relation can be affected. Therefore, it is necessary to use the multiple nonlinear regression model to establish the nonlinear response relationship between the deformation and external factors [44–48]. The multiple nonlinear regression model can be expressed as follows:

$$y_2 = a_1x_1 + \dots + a_nx_n + b_1x_1^2 + \dots + b_nx_n^2 + c \quad (2)$$

where y_2 represents the predicted result of using the multiple nonlinear regression model, $x_1, x_2 \dots x_n$ are the factors that affect the slope deformation, a_1, a_2, \dots, a_n and b_1, b_2, \dots, b_n are the coefficients, and c is the random error.

2.5. Modified Deformation Prediction Combination Model Based on GFW-Fisher Optimal Segmentation Method

In this study, the slope deformation is affected by the human factor, geological factor, environmental factor and other multi-source factors. It is difficult for the single model to accurately predict deformation and data fluctuation is likely to make errors in the processing of predicting deformation, which cannot meet the needs of predicting slope deformation [49,50]. Therefore, we perform the modified combination model of slope deformation prediction to predict slope deformation at different spatial scales, overcome the shortcomings of the single model and the interference of data fluctuation and human factor to improve the prediction accuracy of slope deformation. Briefly, the Fisher optimal segmentation method is used to segment slope deformation at different spatial scales and solve the problem of data fluctuation. The segmented data are used to be predicted using the multiple linear regression model and multiple nonlinear regression model. Meanwhile, GFW model can be used to assign different weights to the multiple linear regression model and multiple nonlinear regression model, which can be used to solve the problem of human factors on the prediction results. The combination model of slope deformation prediction can be established using the linear combination model, weighted geometric average model, and weighted harmonic average model, respectively. The high-accuracy combination model can be used as the chosen prediction model of slope deformation. The process of constructing the prediction combination model is further described in Figure 1, and the steps involved in constructing models are commonly shown as follows:

The matrix A is established by choosing the deformation speed and acceleration at different spatial scales. The matrix A is shown as:

$$A = \begin{bmatrix} x_{11} & \dots & x_{1j} \\ \vdots & \ddots & \vdots \\ x_{i1} & \dots & x_{ij} \end{bmatrix} \tag{3}$$

The matrix A need to be normalized and the process is shown as:

$$A' = \begin{cases} (x_{ij} - x_{min.j}) / (x_{max.j} - x_{min.j}) \\ (x_{min.j} - x_{ij}) / (x_{max.j} - x_{min.j}) \end{cases} \tag{4}$$

where x_{ij} is the i th data of the j th indicator. $x_{min.j}$ is the minimum of the j th indicator. $x_{max.j}$ is the maximum of the j th indicator.

The sequence sample is a completed classification, one of the classifications is set $\{x_i, x_{i+1}, \dots, x_j\}$, and the diameter of the classification is shown as:

$$\begin{cases} \bar{x}_{ij} = \frac{\sum_{t=i}^j x_t}{j-i+1} \\ D(i, j) = \sum_{t=i}^j (x_t - \bar{x}_{ij})^2 \end{cases} \tag{5}$$

where $D(i, j)$ is larger, the internal difference of classification is greater.

The sample is divided into the k classification and the results are shown as: $\{i_1, i_1 + 1, i_1 + 2, \dots, i_2 - 1\}$, $\{i_2, i_2 + 1, i_2 + 2, \dots, i_3 - 1\}$, $\{i_k, i_k + 1, i_k + 2, \dots, i_{k+1} - 1\}$.

Additionally, the error function is set as: $E[F(n, k)] = \sum_{j=i}^k D(j_1, j_{i+1} - 1)$. When n and

k are determined, the value of error function is smaller, the sum of internal diameter is smaller, and the classification is more reasonable. When the minimum of the error function is $E(F \times (n, k))$, and the k of the inflection point where the drawing $E(F \times (n, k)) \sim k$ related curve is more obvious is the optimal number of classifications.

The k-class data are predicted using the multiple linear regression model and multiple nonlinear regression model and the fitting degree of the two models is computed, respectively. The fitting degree is shown as:

$$R_1^2 = \frac{\sum(y_1 - \bar{y})^2}{\sum(y - \bar{y})^2} \quad (6)$$

$$R_2^2 = \frac{\sum(y_2 - \bar{y})^2}{\sum(y - \bar{y})^2} \quad (7)$$

where y is the original sample sequence, \bar{y} is the average of the original sample sequence, y_1 is the fitting of the multiple linear regression model, and y_2 is the fitting of the multiple nonlinear regression model. Meanwhile, the range of R^2 is between zero and one. Therefore, when R^2 is closer to one, the reference value of the relevant model is higher. On the contrary, the reference value of the relevant model is lower.

The weights of two models are assigned by constructing the GFW model, which is shown as:

$$w_1 = \frac{R_1^2}{R_1^2 + R_2^2} \quad (8)$$

$$w_2 = 1 - w_1 \quad (9)$$

where w_1 is the weight of the multiple linear regression model, and w_2 is the weight of multiple nonlinear regression model.

The combination model is established by choosing the linear combination model, weighted geometric average model and weighted harmonic average model, respectively. The combination model is shown as:

$$y_3 = w_1 y_1 + w_2 y_2 \quad (10)$$

$$y_4 = y_1^{w_1} \times y_2^{w_2} \quad (11)$$

$$y_5 = \frac{y_1 \times y_2}{w_1 y_1 + w_2 y_2} \quad (12)$$

where y_3 is the prediction results of the linear combination model, y_4 is the prediction results of the weighted geometric average model, and y_5 is the prediction results of the weighted harmonic average model.

In summary, we used the modified prediction combination model based on the GFW-Fisher optimal segmentation method to establish the slope deformation prediction model, and used Fisher optimal segmentation method to solve the influence of data fluctuation. Meanwhile, we also used the combination model to solve the influence of human factors, and made the prediction results more accurate.

2.6. Model Accuracy Evaluation

On the basis of the construction of slope deformation prediction combination model, it is necessary to further evaluate the applicability of the model. In this study, the Root Mean Squared Error (RMSE), Mean Absolute Error (MAE) and Relative Error (RE) were used as the evaluation indicators to verify the accuracy of the model. The process of calculating the indicators is shown as:

$$\text{RMSE} = \sqrt{\frac{1}{N} \sum_{i=1}^N (y - \hat{y})^2} \quad (13)$$

$$\text{MAE} = \frac{1}{N} \sum_{i=1}^N |(y - \hat{y})| \quad (14)$$

$$RE = \frac{|y - \hat{y}|}{y} \times 100\% \quad (15)$$

where y is the prediction results of the combination model, \hat{y} is the actual results of slope deformation, and N is the number of sample data.

3. Results and Discussion

In this study, we performed the experiments in Red Rock Slope by selecting the deformation of the high slope DEM model at different spatial scales of point, linear, and surface under 100 grids and 200 grids from 1 January 2019 to 31 December 2019. The modified combination model of slope deformation prediction was established using the GFW-Fisher optimal segmentation model. The prediction results of various combination models were analyzed, and the accuracy evaluation of the model was completed.

3.1. Slope Deformation Prediction Results

Slope deformation was mainly affected by the geological factor, climatic factor, and human factor at different spatial scales, which makes deformation data have large fluctuations at different times. Thus, the Fisher optimal segmentation method was used to segment the sample data by combining speed with acceleration at different spatial scales, and solve the influence of data fluctuation on the slope deformation prediction results. The results of the data segmentation with the Fisher optimal segmentation are shown in Figure 3.

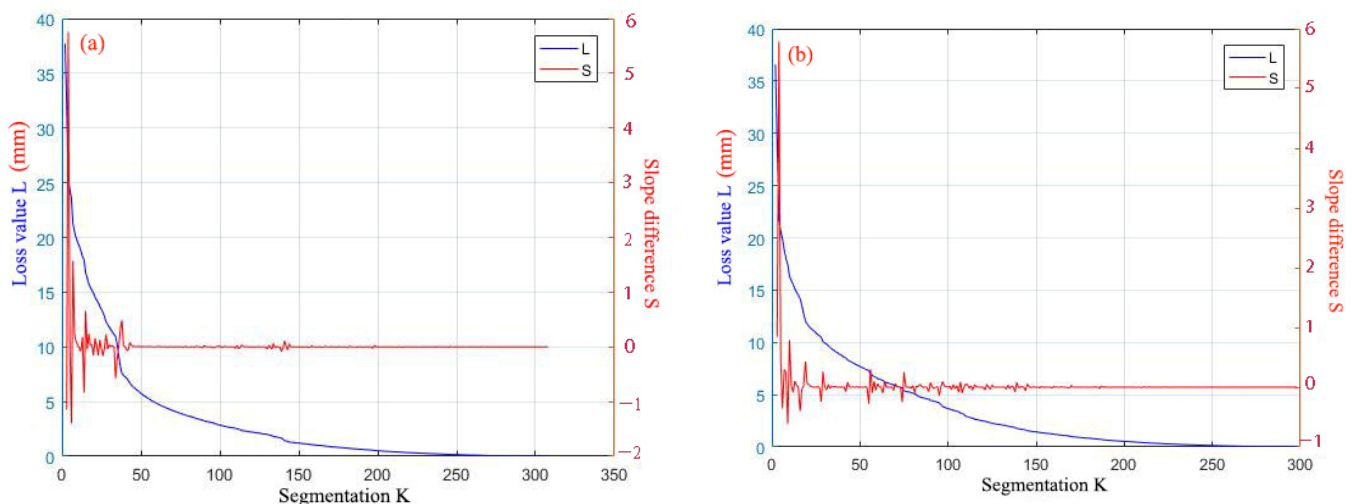


Figure 3. The results of Fisher optimal segmentation method under the different number of grids. (a) 100 grids; (b) 200 grids.

Figure 3a,b shows that the results were obtained from the Fisher optimal segmentation model under 100 grids and 200 grids, respectively. The flexion points of the results under different numbers of grids were clear when k was four, the slope difference presented by red reached peak, the optimal number of sample segmentation should be four, and the loss value presented by blue is the value corresponding to the slope difference.

The segmented data were used for prediction by using the multiple linear regression model and multiple nonlinear regression model after completing the segmentation of data at different spatial scales, respectively. Additionally, two models were assigned different weights by constructing the GFW model. The weights of the segmented data at different spatial scales are shown in Table 1.

Table 1. The weights assigned by the goodness-of-fit weight model.

Spatial and Scale	Intervals	Weights of Multiple Linear Regression Model	Weights of Multiple Nonlinear Regression Model
Deformation prediction at point scales with 100 grids	The first interval	0.594	0.406
	The second interval	0.205	0.795
	The third interval	0.813	0.187
	The fourth interval	0.322	0.678
Deformation prediction at linear scales with 100 grids	The first interval	0.256	0.744
	The second interval	0.090	0.910
	The third interval	0.369	0.631
	The fourth interval	0.415	0.585
Deformation prediction at surface scales with 100 grids	The first interval	0.198	0.802
	The second interval	0.060	0.940
	The third interval	0.440	0.560
	The fourth interval	0.076	0.924
Deformation prediction at point scales with 200 grids	The first interval	0.426	0.574
	The second interval	0.228	0.772
	The third interval	0.330	0.670
	The fourth interval	0.654	0.346
Deformation prediction at linear scales with 200 grids	The first interval	0.184	0.816
	The second interval	0.358	0.642
	The third interval	0.454	0.546
	The fourth interval	0.312	0.688
Deformation prediction at surface scales with 200 grids	The first interval	0.727	0.273
	The second interval	0.117	0.883
	The third interval	0.366	0.634
	The fourth interval	0.366	0.634

The multiple linear regression model and multiple nonlinear regression model were combined using the linear combination model, weighted geometric average model and weighted harmonic average model, respectively. Then the combination model of slope deformation prediction based on the GFW-Fisher optimal segmentation method was established. Meanwhile, we obtained the combination results of 18 groups through experiments and selected the appropriate prediction combination model by comparing the determination coefficients of the combination results. The results of the prediction combination models are shown in Figure 4.

Tables 2 and 3 show that the determination coefficients between the prediction results and actual results of the modified combination model were strong, and the grids were more and the determination coefficients were higher. When the number of grids in the DEM model were same, the determination coefficients between the prediction results and actual results at surface scales were the highest. Therefore, we should choose the weighted harmonic average model as the prediction combination model of slope deformation at the surface scale under 200 grids from the combination results from 18 groups.

Table 2. Determination coefficients (R^2) of the modified slope deformation prediction model at different spatial scales with 100 grids.

Spatial Scale	Linear Combination Model	Weighted Geometric Average Model	Weighted Harmonic Average Model
Point scale	0.89	0.88	0.83
Linear scale	0.77	0.79	0.84
Surface scale	0.93	0.93	0.95

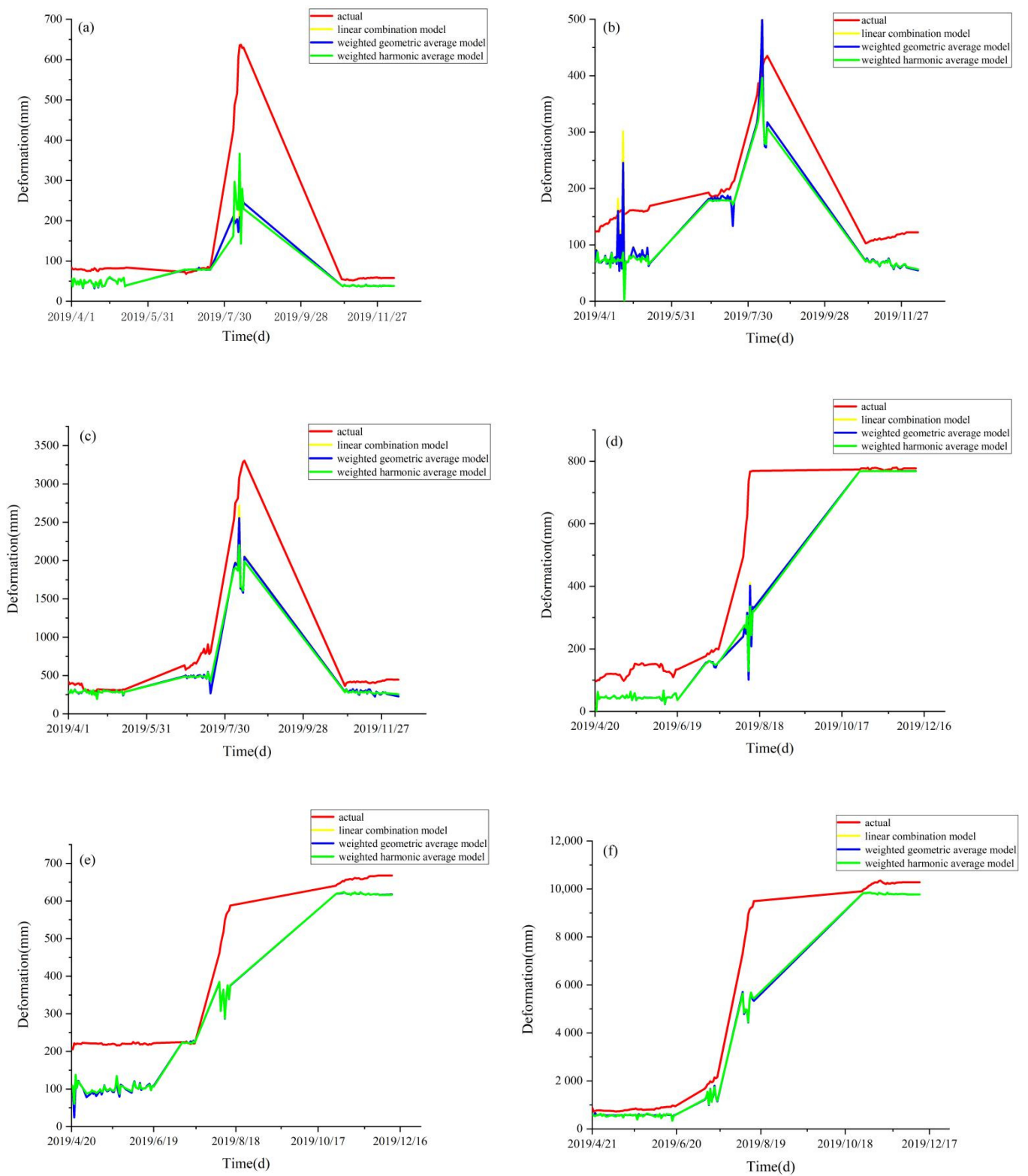


Figure 4. The results of the different prediction combination model at different spatial scales with the different number of grids. (a) Point scale and 100 grids; (b) linear scale and 100 grids; (c) surface scale and 100 grids; (d) point scale and 200 grids; (e) linear scale and 200 grids; and (f) surface scale and 200 grids.

Table 3. Determination coefficients (R^2) of the modified slope deformation prediction model at different spatial scales with 200 grids.

Spatial Scale	Linear Combination Model	Weighted Geometric Average Model	Weighted Harmonic Average Model
Point scale	0.88	0.87	0.88
Linear scale	0.94	0.94	0.94
Surface scale	0.95	0.95	0.96

Figure 5 shows the prediction results of different models. This could be explained by the fact that the prediction result of the modified combination model was great, the determination coefficient was closer to one, and the fitting degree was strong. However, the determination coefficient of the multiple linear regression model and multiple nonlinear regression model were 0.15279 and 0.19802, respectively, and the prediction capacities of two models were terrible. This was the main problem of the existing data fluctuation and it could not be considered using the multiple linear regression model and multiple nonlinear regression model to predict slope deformation. For example, the surface deformation on 19 June 2019 and 20 June 2019 was 944.95 mm and 980.11 mm, respectively, and the results of data fluctuation was 35.16 mm. The surface deformation on 19 July 2019 and 20 July 2019 was 2164.63 mm and 2522.87 mm, respectively, and the results of data fluctuation was 358.24 mm. The surface deformation on 14 August 2019 and 15 August 2019 were 9492.75 mm and 9527.14 mm, respectively, and the results of data fluctuation was 34.49 mm. Therefore, our results also verified that slope deformation could not be predicted accurately under the problem of data fluctuation. Additionally, the problem was solved using the modified combination model of deformation prediction based on the GFW-Fisher optimal segmentation method, and the accuracy of predicting was improved.

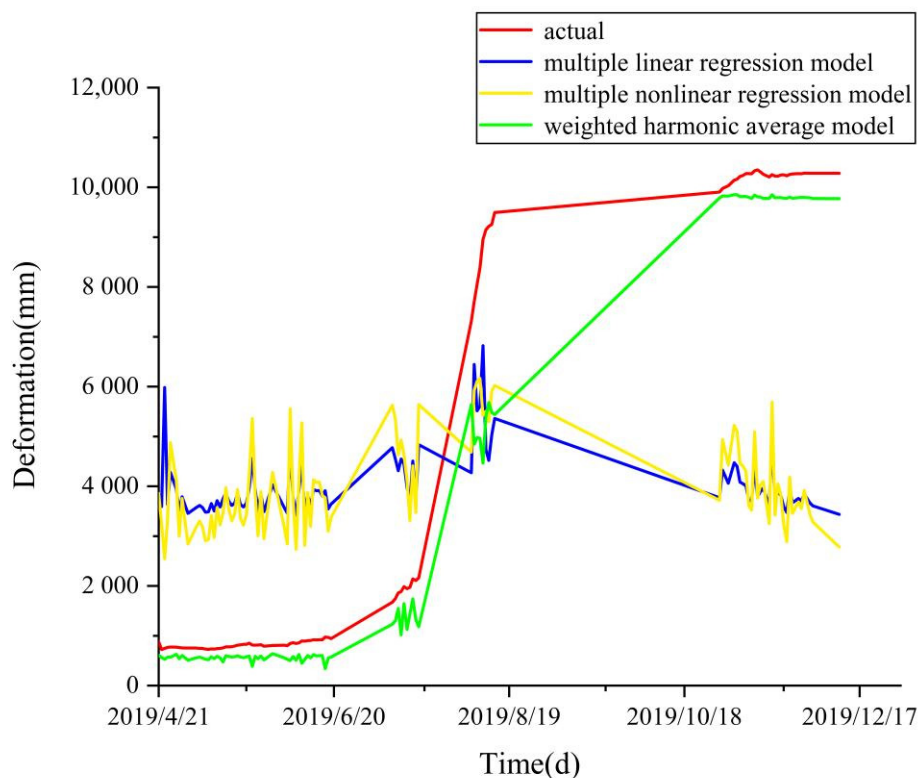


Figure 5. The comparing results of combination model, multiple linear regression model, and multiple nonlinear regression model.

3.2. The Results of Accuracy Evaluation

In order to further verify the applicability of the modified model, it is necessary to evaluate the accuracy of the model. Therefore, 70 percent of the sample data could be used to establish the evaluation model and 30 percent of the sample data could be used to evaluate the accuracy. RMSE, MAE and relative error could be used as the evaluation indicators to evaluate the accuracy of the model at different spatial scales under different numbers of grids. However, the obtained remote sensing images could be characterized using the high-resolution ratio, so the error between the prediction results and actual results should be distributed to each grid. Meanwhile, the accuracy of the multiple linear regression model, multiple nonlinear regression model and combination model should be evaluated by comparing the indicators of the traditional model and modified model. The results of the accuracy evaluation are shown in Table 4.

Table 4. The evaluation results of the model accuracy.

Model	RMSE	MAE	Relative Error
Multiple linear regression model	20.91%	19.52%	96.33%
Multiple nonlinear regression model	20.74%	19.14%	94.47%
Linear combination model	5.62%	3.14%	4.33%
Weight geometric average model	5.62%	3.12%	4.33%
Weight harmonic average model	5.57%	3.11%	3.98%

Table 4 shows that the values of RMSE, MAE and relative error of the weighted harmonic average model are smaller than other combination models. Therefore, the capacity to predict and fit the weighted harmonic average model should be stronger than a single model. Meanwhile, these indicators could be used to evaluate the errors between prediction results and actual results, which could be distributed to each grid. Additionally, the weight harmonic average model should be used as the prediction model.

3.3. Discussion

The methodology in this study has a number of distinctive characteristics in relation to the prediction model in the field of slope collapse. The method takes many environment and climate impacts, across a range of sectors, into consideration. The extensive slope deformation data are systematically collected, which is a scientific and reliable data resource enabling deformation prediction. The slope deformation data used here are mainly from Ground-based Synthetic Aperture Radar. In addition, we considered not only the disadvantage of the single prediction model but also the impacts of data fluctuation. Finally, the deformation prediction at different spatial scales with different scales was explored using the approach proposed, and the accuracy of the model was used to assess by indicators such as MAE, RMSE, and relative error.

For the accuracy of the model proposed by our study, the results showed that the combination model was more accurate than the single model. The most accurate combination model was the weight harmonic average model, thus indicating that it should be used as the appropriate model to predict slope deformation. This is consistent with existing research by Tan et al., which established a model in consideration of the relevance of the multi-point space to predict slope deformation [51]. Du et al. used the model to predict slope deformation and found that the combination model was more accurate and reliable than the single point model [52]. Their results showed that the combination model had a higher prediction capacity, and the determination of the coefficient of the combination model by their study was 0.95. The results presented in our study identified the weight harmonic average model as having the highest prediction capacity, and the determination of the coefficient of the combination model in our study was 0.96. Clearly, the stability of the results obtained using our proposed method is stronger than their method. They collected slope deformation data and used the combination model to predict the slope deformation, which were mainly restricted to the small scale and the single spatial scale. In

contrast to their results, our results are based on the consideration of data fluctuation and human factors, which had been applied to the different spatial scales such as point, line and surface and larger scales. For this reason, our method has a better capacity than other methods for deformation prediction.

In summary, we established the combination prediction model as a novel method of slope deformation prediction, which improved the accuracy of the prediction results. The results from our proposed model revealed the difference in prediction results at different spatial scales and different scales. The weight harmonic average model at the surface scale with a large scale should be used as the appropriate combination model, which can provide a scientific reference for the safety of water projects.

4. Conclusions

Unlike traditional prediction methods for slope deformation, a new method has been proposed to predict the slope deformation at different spatial scales. The method successfully identified the prediction results of the slope deformation at different scales by establishing the modified combination model and selected the appropriate combination model as the deformation prediction model. Meanwhile, this study used the model to undertake experiments in 2019. We used this method to predict the deformation of the high slope at different spatial scales, which could solve the interference of data fluctuation and human factor to a great extent and improve the accuracy of the deformation prediction. We concluded that the determination coefficient of the weighted harmonic average model was the highest with a surface scale with 200 grids, and the stability of weighted harmonic average model was stronger than other combination models. Meanwhile, the stability of the proposed combination model at the same spatial scale with 200 grids was stronger than 100 grids. Therefore, the weighted harmonic average model should be used as the slope deformation prediction combination model when the scale is a surface scale with 200 grids. Our experimental results revealed that the capacity of predicting and fitting of improved combination model was greater than traditional model by establishing an improved prediction combination model based on the GFW-Fisher optimal segmentation method. The RMSE, MAE and relative error have been significantly improved, which may be effectively reflected by the slope deformation and provide the reference for ensuring the safe construction of water engineering.

This study objectively reports that the improved combination model has solved the disadvantage of the single model and the accuracy of predicting the improved combination model is greater than the traditional model. However, future work will be required to verify the stability of the combination model for the high slope with more time scales such as hour and minute. Additionally, our proposed method should be used and implemented within other geological conditions.

Author Contributions: Data analysis, T.L.; formal analysis, X.L., J.W. and D.C.; funding acquisition, J.Q., G.Q. and W.W.; investigation T.L.; methodology, X.L. and D.C.; validation, T.L., J.W. and X.L.; writing—original draft preparation, X.L.; writing—review and editing, J.L. and T.L. All authors have read and agreed to the published version of the manuscript.

Funding: The study was financially supported by the Agricultural Science and Technology Innovation Program of Chinese Academy of Agricultural Sciences.

Data Availability Statement: Data available on request due to restrictions eg privacy or ethical. The data presented in this study are available on request from the corresponding author. The data are not publicly available due to the signing of a non-disclosure agreement.

Acknowledgments: We acknowledge reviewers who helped us in the review process.

Conflicts of Interest: The authors declare no conflict of interest.

References

1. Singh, P.; Gupta, A.; Singh, M. Hydrological inferences from watershed analysis for water resource management using remote sensing and GIS techniques. *Egypt. J. Remote Sens. Space Sci.* **2014**, *17*, 111–121. [\[CrossRef\]](#)
2. Salifu, E.; MacLachlan, E.; Iyer, K.R.; Knapp, C.W.; Tarantino, A. Application of microbially induced calcite precipitation in erosion mitigation and stabilisation of sandy soil foreshore slopes; a preliminary investigation. *Eng. Geol.* **2016**, *201*, 96–105. [\[CrossRef\]](#)
3. Zhong, B.; Peng, S.; Zhang, Q.; Ma, H.; Cao, S. Using an ecological economics approach to support the restoration of collapsing gullies in southern China. *Land Use Policy* **2013**, *32*, 119–124. [\[CrossRef\]](#)
4. Zhang, X.; Nie, J.; Cheng, C.; Xu, C.; Zhou, L.; Shen, S.; Pei, Y. Natural and Socioeconomic Factors and Their Interactive Effects on House Collapse Caused by Typhoon Mangkhut. *Int. J. Disaster Risk Sci.* **2021**, *12*, 121–130. [\[CrossRef\]](#)
5. Che, A.; Yang, H.; Wang, B.; Ge, X. Wave propagations through jointed rock masses and their effects on the stability of slopes. *Eng. Geol.* **2016**, *201*, 45–56. [\[CrossRef\]](#)
6. Cheng, M.; Hoang, N. A Swarm-Optimized Fuzzy Instance-based Learning approach for predicting slope collapses in mountain roads. *Knowl.-Based Syst.* **2015**, *76*, 256–263. [\[CrossRef\]](#)
7. Dick, G.J.; Eberhardt, E.; Cabrejo-Liévano, A.G.; Stead, D.; Rose, N.D. Development of an early-warning time-of-failure analysis methodology for open-pit mine slopes utilizing ground-based slope stability radar monitoring data. *Can. Geotech. J.* **2015**, *52*, 515–529. [\[CrossRef\]](#)
8. Xu, J.; Li, H.; Du, K.; Yan, C.; Zhao, X.; Li, W.; Xu, X. Field investigation of force and displacement within a strata slope using a real-time remote monitoring system. *Environ. Earth Sci.* **2018**, *77*, 1–11. [\[CrossRef\]](#)
9. He, Z.; Xie, M.; Huang, Z.; Lu, G.; Yan, B.; Wang, J. Method to Realize the Tilt Monitoring and Instability Prediction of Hazardous Rock on Slopes. *Adv. Civ. Eng.* **2021**, *2021*, 1–14. [\[CrossRef\]](#)
10. Mazzanti, P.; Bozzano, F.; Cipriani, I.; Prestininzi, A. New insights into the temporal prediction of landslides by a terrestrial SAR interferometry monitoring case study. *Landslides* **2015**, *12*, 55–68. [\[CrossRef\]](#)
11. Li, M.; Zhang, L.; Ding, C.; Li, W.; Luo, H.; Liao, M.; Xu, Q. Retrieval of historical surface displacements of the Baige landslide from time-series SAR observations for retrospective analysis of the collapse event. *Remote Sens. Environ.* **2020**, *240*, 111695. [\[CrossRef\]](#)
12. Dong, M.; Wu, H.; Hu, H.; Azzam, R.; Zhang, L.; Zheng, Z.; Gong, X. Deformation Prediction of Unstable Slopes Based on Real-Time Monitoring and DeepAR Model. *Sensors* **2020**, *21*, 14. [\[CrossRef\]](#)
13. Jiang, S.; Lian, M.; Lu, C.; Gu, Q.; Ruan, S.; Xie, X. Ensemble Prediction Algorithm of Anomaly Monitoring Based on Big Data Analysis Platform of Open-Pit Mine Slope. *Complexity* **2018**, *2018*, 1–13. [\[CrossRef\]](#)
14. Hu, B.; Su, G.; Jiang, J.; Sheng, J.; Li, J. Uncertain Prediction for Slope Displacement Time-Series Using Gaussian Process Machine Learning. *IEEE Access* **2019**, *7*, 27535–27546. [\[CrossRef\]](#)
15. Zhang, Y.-G.; Tang, J.; He, Z.-Y.; Tan, J.; Li, C. A novel displacement prediction method using gated recurrent unit model with time series analysis in the Erdaohe Landslide. *Nat. Hazards* **2021**, *10*, 783–813. [\[CrossRef\]](#)
16. Khajezadeh, M.; Taha, M.R.; Keawsawasvong, S.; Mirzaei, H.; Jebeli, M. An Effective Artificial Intelligence Approach for Slope Stability Evaluation. *IEEE Access* **2022**, *10*, 5660–5671. [\[CrossRef\]](#)
17. Zhao, X.; Ye, S. Space reconstruction of audiovisual media based on artificial intelligence and virtual reality. *J. Intell. Fuzzy Syst.* **2021**, *40*, 7285–7296. [\[CrossRef\]](#)
18. Zhang, H.; Nguyen, H.; Bui, X.-N.; Pradhan, B.; Asteris, P.G.; Costache, R.; Aryal, J. A generalized artificial intelligence model for estimating the friction angle of clays in evaluating slope stability using a deep neural network and Harris Hawks optimization algorithm. *Eng. Comput.* **2021**, 1–14. [\[CrossRef\]](#)
19. Huang, Y.; Han, X.; Zhao, L. Recurrent neural networks for complicated seismic dynamic response prediction of a slope system. *Eng. Geol.* **2021**, *289*, 106198. [\[CrossRef\]](#)
20. Elsheikh, A.H.; Panchal, H.; Ahmadein, M.; Mosleh, A.O.; Sadasivuni, K.K.; Alsaleh, N.A. Productivity forecasting of solar distiller integrated with evacuated tubes and external condenser using artificial intelligence model and moth-flame optimizer. *Case Stud. Therm. Eng.* **2021**, *28*, 101671. [\[CrossRef\]](#)
21. Yang, B.; Yin, K.; Lacasse, S.; Liu, Z. Time series analysis and long short-term memory neural network to predict landslide displacement. *Landslides* **2019**, *16*, 677–694. [\[CrossRef\]](#)
22. Ozsen, H. Monitoring unstable slopes in an open pit lignite mine using ARIMA. *J. S. Afr. Inst. Min. Metall.* **2020**, *120*, 173–180. [\[CrossRef\]](#)
23. Gong, C.; Lei, S.; Bian, Z.; Tian, Y.; Zhang, Z.; Guo, H.; Zhang, H.; Cheng, W. Using time series InSAR to assess the deformation activity of open-pit mine dump site in severe cold area. *J. Soil. Sediment.* **2021**, *21*, 3717–3732. [\[CrossRef\]](#)
24. Momeni, E.; Yarivand, A.; Dowlatshahi, M.B.; Armaghani, D.J. An efficient optimal neural network based on gravitational search algorithm in predicting the deformation of geogrid-reinforced soil structures. *Transp. Geotech.* **2021**, *26*, 100446. [\[CrossRef\]](#)
25. Barvor, Y.J.; Bacha, S.; Qingxiang, C.; Zhao, C.S.; Siddique, M. Surface mines composite slope deformation mechanisms and stress distribution. *Min. Miner. Depos.* **2020**, *14*, 1–16. [\[CrossRef\]](#)
26. Deng, L.; Smith, A.; Dixon, N.; Yuan, H. Machine learning prediction of landslide deformation behaviour using acoustic emission and rainfall measurements. *Eng. Geol.* **2021**, *293*, 106315. [\[CrossRef\]](#)

27. Li, L.; Qiang, Y.; Li, S.; Yang, Z. Research on Slope Deformation Prediction Based on Fractional-Order Calculus Gray Model. *Adv. Civ. Eng.* **2018**, *2018*, 1–9. [[CrossRef](#)]
28. Bacha, S.; Barvor, Y.J.; Qingxiang, C.; Zhao, C.S.; Wang, M. Influence of composite slope geometrical parameters on soft rock slope stability. *Min. Miner. Depos.* **2020**, *14*, 112–119. [[CrossRef](#)]
29. Abdellah, W.R.; Hussein, M.Y.; Imbabi, S.S. Rock slope stability analysis usingshear strength reduction technique (SSRT)–Case histories. *Min. Miner. Depos.* **2020**, *14*, 16–24. [[CrossRef](#)]
30. Jiang, N.; Li, H.; Zhou, J. Quantitative hazard analysis and mitigation measures of rockfall in a high-frequency rockfall region. *Bull. Eng. Geol. Environ.* **2021**, *80*, 3439–3456. [[CrossRef](#)]
31. Luo, D.; Li, H.; Wu, Y.; Li, D.; Yang, X.; Yao, Q. Cloud model-based evaluation of landslide dam development feasibility. *PLoS ONE* **2021**, *16*, e0251212. [[CrossRef](#)]
32. Jiang, F.; Dai, X.; Xie, Z.; Xu, T.; Yin, S.; Qu, G.; Yang, S.; Zhang, Y.; Yang, Z.; Xu, J.; et al. Flood inundation evolution of barrier lake and evaluation of regional ecological spatiotemporal response—a case study of Sichuan-Tibet region. *Environ. Sci. Pollut. Res.* **2022**, *29*, 71290–71310. [[CrossRef](#)] [[PubMed](#)]
33. Su, X.; Ma, S.; Qiu, X.; Shi, J.; Zhang, X.; Chen, F. Microblog Topic-Words Detection Model for Earthquake Emergency Responses Based on Information Classification Hierarchy. *Int. J. Environ. Res. Public Health* **2021**, *18*, 8000. [[CrossRef](#)] [[PubMed](#)]
34. Sun, X.; Guo, L. Crustal velocity, density structure, and seismogenic environment in the southern segment of the North-South Seismic Belt, China. *Earthq. Sci.* **2021**, *34*, 471–488. [[CrossRef](#)]
35. Lv, M.; Ding, Z.; Xu, X. Seismogenic environments of earthquakes on the southeastern margin of the Tibetan Plateau revealed by double-difference tomography. *Tectonophysics* **2022**, *843*, 229603. [[CrossRef](#)]
36. Lu, X.; Cheng, Q.; Xu, Z.; Xiong, C. Regional seismic-damage prediction of buildings under mainshock-aftershock sequence. *Front. Eng. Manag.* **2021**, *8*, 122–134. [[CrossRef](#)]
37. Jiang, P.; Li, R.; Liu, N. A novel composite electricity demand forecasting framework by data processing and optimized support vector machine. *Appl. Energy* **2020**, *260*, 114243. [[CrossRef](#)]
38. Zhang, L.; Cai, X.; Wang, Y.; Wei, W.; Liu, B.; Jia, S.; Pang, T.; Bai, F.; Wei, Z. Long-term ground multi-level deformation fusion and analysis based on a combination of deformation prior fusion model and OTD-InSAR for longwall mining activity. *Meas. J. Int. Meas. Confed.* **2020**, *161*, 107911. [[CrossRef](#)]
39. Ottaviani, M.F.; Marco, A.D. Multiple Linear Regression Model for Improved Project Cost Forecasting. *Procedia Comput. Sci.* **2022**, *196*, 808–815. [[CrossRef](#)]
40. Babar, I.; Ayed, H.; Chand, S.; Suhail, M.; Khan, Y.A.; Marzouki, R. Modified Liu estimators in the linear regression model: An application to Tobacco data. *PLoS ONE* **2021**, *16*, e0259991. [[CrossRef](#)] [[PubMed](#)]
41. Yang, K.; Musselman, K.N.; Rittger, K.; Margulis, S.A.; Painter, T.H.; Molotch, N.P. Combining ground-based and remotely sensed snow data in a linear regression model for real-time estimation of snow water equivalent. *Adv. Water Resour.* **2022**, *160*, 104075. [[CrossRef](#)]
42. Tang, S.; Li, T.; Guo, Y.; Zhu, R.; Qu, H. Correction of various environmental influences on Doppler wind lidar based on multiple linear regression model. *Renew. Energy* **2022**, *184*, 933–947. [[CrossRef](#)]
43. Roozbeh, M.; Babaie-Kafaki, S.; Aminifard, Z. A nonlinear mixed-integer programming approach for variable selection in linear regression model. *Communications in statistics. Simul. Comput.* **2021**, 1–12, *ahead of print*. [[CrossRef](#)]
44. Jahangir, H.; Bagheri, M.; Delavari, S.M.J. Cyclic Behavior Assessment of Steel Bar Hysteretic Dampers Using Multiple Nonlinear Regression Approach. *Iranian journal of science and technology. Trans. Civ. Eng.* **2021**, *45*, 1227–1251.
45. Cepowski, T.; Chorab, P.; Łozowicka, D. Application of an Artificial Neural Network and Multiple Nonlinear Regression to Estimate Container Ship Length Between Perpendiculars. *Pol. Marit. Res.* **2021**, *28*, 36–45. [[CrossRef](#)]
46. Zhang, K.; Li, W.; Han, Y.; Geng, Z.; Chu, C. Production capacity identification and analysis using novel multivariate nonlinear regression: Application to resource optimization of industrial processes. *J. Clean. Prod.* **2021**, *282*, 124469. [[CrossRef](#)]
47. Basco, R.; Hair, J.F.; Ringle, C.M.; Sarstedt, M. Advancing family business research through modeling nonlinear relationships: Comparing PLS-SEM and multiple regression. *J. Fam. Bus. Strategy* **2022**, *13*, 100457. [[CrossRef](#)]
48. Kun, Z.; Weibing, F. Prediction of China’s Total Energy Consumption Based on Bayesian ARIMA-Nonlinear Regression Model. *IOP conference series. Earth Environ. Sci.* **2021**, *657*, 12056.
49. Zhang, W.; Xiao, R.; Shi, B.; Zhu, H.-H.; Sun, Y.-J. Forecasting slope deformation field using correlated grey model updated with time correction factor and background value optimization. *Eng. Geol.* **2019**, *260*, 105215. [[CrossRef](#)]
50. Cai, M.; Koopialipour, M.; Armaghani, D.J.; Pham, B.T. Evaluating Slope Deformation of Earth Dams Due to Earthquake Shaking Using MARS and GMDH Techniques. *Appl. Sci.* **2020**, *10*, 1486. [[CrossRef](#)]
51. Tan, X.L. Combinatorial Method of Deformation Prediction Based on Multipoint Monitoring for Large Slope and Its Engineering Application. *J. Yangtze River Sci. Res. Inst.* **2014**, *31*, 143–148.
52. Du, S.; Zhang, J.; Deng, Z.; Li, J. A New Approach of Geological Disasters Forecasting using Meteorological Factors based on Genetic Algorithm Optimized BP Neural Network. *Elektron. Ir Elektrotehnika* **2014**, *20*, 57–62. [[CrossRef](#)]